

# Time Asymmetry of Cosmic Background Evolution in Loop Quantum Cosmology

Wen-Hsuan Lucky Chang and Jiun-Huei Proty Wu

*Department of Physics, Institute of Astrophysics, and Center for Theoretical Physics,  
National Taiwan University, Taipei 10617, Taiwan*

We discuss the asymmetry of cosmic background evolution in time with respect to the quantum bounce in the Loop Quantum Cosmology (LQC), employing the newly proposed bouncing parameter  $\alpha_s$ . We use the Chaotic and the  $R^2$  potentials to demonstrate that a possible deflation before the bounce may counteract the inflation that is needed for resolving the cosmological conundrums, so a certain level of time asymmetry is required for the models in LQC. This  $\alpha_s$  is model dependent and closely related to the amounts of deflation and inflation, so we may use observations to confine  $\alpha_s$  and thus the model parameters. With further studies this formalism should be useful in providing an observational testbed for the LQC models.

## I. INTRODUCTION

Singularity at the beginning of spacetime is a long-standing problem in cosmology [1]. One solution is to consider the Loop Quantum Cosmology (LQC), which is a theory of Loop Quantum Gravity (LQG) simplified with the cosmological principle [2]. It employs the Friedmann-Robertson-Walker (FRW) model with quantum corrections. The extra terms involve a scalar field to resolve the singularity problem with a quantum bounce [3]. In turn this allows for the existence of a ‘parent universe’ [4–6].

To evolve the scale factor under this context, the quantum corrected Friedmann equation [7, 8] was derived with the Hamiltonian formulation in a semi-classical approach [9]. Two major types of quantum corrections are the holonomy [10–12] and the inverse volume [13]. The Hamiltonian involves the connection variables (known as the Ashtekar variables in LQC), whose equations of motion can be obtained by calculating their Poisson brackets. Because these connection variables are actually functions of the scale factor and the Hubble parameter, we could eventually obtain the evolution equation of the scale factor.

Within the LQC framework, inflation occurs naturally after the quantum bounce due to the existence of a scalar field [14], so that the cosmological conundrums can be resolved in the conventional way [15]. Before the quantum bounce this scalar field may also generate a period of damped contraction called ‘deflation’. The amount of deflation and that of inflation may differ and one key is the potential to kinetic energy ratio (PKR) of the scalar field at the quantum bounce. Here we shall propose a more intuitive ‘bouncing parameter’ to study the asymmetry between deflation and inflation.

This paper investigates in details the dependence of cosmic time asymmetry on the bouncing parameter. The two inflationary models considered here are the Chaotic potential (a commonly chosen simple model) and the  $R^2$  potential (a realistic model to date [16]).

Here is the structure of this paper. First we lay out our convention of LQC in Section II, where Section II A defines the Hamiltonian formalism, with its quantum cor-

rections presented in Section II B. Section III investigates the time asymmetry in cosmic evolution, in particular employing the newly proposed ‘bouncing parameter’. Section IV discusses the possible deflation and its impact. We conclude our work in Section V. The units of all physical quantities in this paper are normalized to the Planckian units ( $c = G = \hbar = k_B \equiv 1$ ) unless otherwise labeled. The curvature constant is also presumed to be zero, which is consistent with the current observational results.

## II. COSMIC DYNAMICS

### A. Hamiltonian formalism

To have a good handle on the quantum mechanical properties of the early universe, we employ the Arnowitt-Deser-Misner (ADM) approach. The Hamiltonian of spacetime is

$$H_{\text{grav}} = -\frac{3}{8\pi\gamma^2}c^2\sqrt{p}, \quad (1)$$

where  $p$  and  $c$  (not the speed of light) are the connection variables, which are related to the scale factor  $a$  and the Hubble parameter  $H$  as [7]

$$|p| = \frac{1}{4}a^2, \quad (2)$$

$$c = \frac{1}{2}\gamma aH, \quad (3)$$

and satisfy the canonical relation [7]

$$[c, p]_{\text{PB}} = \frac{8\pi\gamma}{3}. \quad (4)$$

The subscript ‘PB’ denotes that the calculation rule follows Poisson Bracket rather than the commutation. The Barbero-Immirzi parameter [17, 18]  $\gamma = \log(3)/\sqrt{2}\pi$  can be obtained from the computation of black hole entropy [19]. In Eqs. (2) and (3) we have dropped the curvature parameter of the FRW model and chosen the coordinate

length of the finite-sized cubic cell in LQG to be unity. It is obvious that the energy density of the spacetime

$$\rho_{\text{grav}} = p^{-3/2} H_{\text{grav}} \quad (5)$$

is unbounded when the size of the universe goes to zero ( $a \rightarrow 0$ ).

On the other hand, the Hamiltonian of the inflaton, which is the only content that matters during a single-field inflation, is

$$H_\phi = \frac{\pi_\phi^2}{2p^{3/2}} + p^{3/2} V(\phi), \quad (6)$$

where the scalar field  $\phi$  and its conjugate momentum  $\pi_\phi$  satisfy the canonical relation [11]

$$[\phi, \pi_\phi]_{\text{PB}} = 1. \quad (7)$$

General Relativity (GR) then requires that the total Hamiltonian must be zero at all times:

$$H_{\text{tot}} = H_{\text{grav}} + H_\phi = 0. \quad (8)$$

This is the Hamiltonian constraint, which is commonly used in solving the Einstein equations numerically [20]. Consequently, the equations of motion that describe the dynamics of the universe are

$$\frac{dq}{dt} = [q, H_{\text{tot}}]_{\text{PB}}, \quad (9)$$

where  $q$  represents  $p$ ,  $c$ ,  $\phi$ , or  $\pi_\phi$  [21]. This set of equations are equivalent to the Friedmann equation and the fluid equation.

### B. Holonomy corrections

For the quantum corrections in the above formalism, we adopt a semi-classical approach in LQC [9]. The  $n$ th-order holonomized connection variable  $c_h^{(n)}$  is defined as [11]

$$c_h^{(n)} \equiv \frac{1}{\bar{\mu}} \sum_{k=0}^n \frac{(2k)!}{2^{2k} (k!)^2 (2k+1)} (\sin \bar{\mu} c)^{2k+1}, \quad (10)$$

where  $\bar{\mu} = \sqrt{\Delta/p}$  is the discreteness variable with  $\Delta = 2\sqrt{3}\pi\gamma$  being the standard choice of the area gap in the full theory of LQG [4]. One key feature in LQC is that the connection variable in the standard cosmology has to be replaced by holonomies. Thus the Hamiltonian of spacetime with the holonomy correction up to the  $n$ th-order is [22]

$$H_{\text{grav}, \bar{\mu}}^{(n)} = -\frac{3}{8\pi\gamma^2} (c_h^{(n)})^2 \sqrt{p}. \quad (11)$$

Finally the new Hamiltonian constraint is [22, 23]

$$H_{\bar{\mu}}^{(n)} = H_{\text{grav}, \bar{\mu}}^{(n)} + H_\phi = 0. \quad (12)$$

We can apply this to the semi-classical approach as what was done in GR [24].

With such quantum corrections, it is obvious that the energy density of the spacetime  $\rho_{\text{grav}}$  is always finite. The extreme values appear when  $\bar{\mu}c$  equals 0,  $\pi/2$ , or its multiples. When  $\bar{\mu}c = \pi/2$ , the Hamiltonian  $H_{\text{grav}, \bar{\mu}}^{(n)}$  reaches its minimum and thus  $H_\phi$  reaches its maximum. The maximal energy density of the inflaton  $\rho_\phi = p^{-3/2} H_\phi$  is called the ‘critical energy density’ and is related to the holonomies as [11]

$$\rho_c^{(n)} = \frac{\sqrt{3}m_{\text{pl}}^4}{16\pi^2\gamma^3} \left[ \sum_{k=0}^n \frac{(2k)!}{2^{2k} (k!)^2 (2k+1)} \right]^2, \quad (13)$$

which is confined between  $\rho_c^{(0)} \simeq 0.82m_{\text{pl}}^4$  and  $\rho_c^{(\infty)} \simeq 2.02m_{\text{pl}}^4$ . We note that the standard cosmology is recovered ( $c_h^{(n)} \rightarrow c$ ) when  $\bar{\mu}c \rightarrow 0$  (that is, when  $p \gg 1$ ). This indicates that the quantum effects are important only when the universe is tiny ( $p \sim \Delta$ ).

Consequently the equations of motion can be obtained as

$$\frac{dq}{dt} = [q, H_{\bar{\mu}}^{(n)}]_{\text{PB}}, \quad (14)$$

which are equivalent to the Friedmann equation and the fluid equation with quantum corrections [7, 8].

## III. COSMIC TIME ASYMMETRY

### A. The Bouncing Scenario

As we have seen in the previous section, the energy density of the scalar field now has a maximum  $\rho_c^{(n)}$  (when  $\bar{\mu}c = \pi/2$ ) and thus avoids the singularity. To see how this is manifested in the behavior of cosmic expansion, we can use the equations of motion to first obtain the Hubble parameter as [22]

$$\begin{aligned} H &= \frac{\dot{a}}{a} = \frac{2}{p} [p, H_{\bar{\mu}}^{(n)}]_{\text{PB}} \\ &= \frac{4}{\gamma\sqrt{p}} \cos(\bar{\mu}c) \mathcal{O}_n(\bar{\mu}c) c_h^{(n)}, \end{aligned} \quad (15)$$

where

$$\mathcal{O}_n(\bar{\mu}c) \equiv \sum_{k=0}^n \frac{(2k)!}{2^{2k} (k!)^2} (\sin \bar{\mu}c)^{2k}. \quad (16)$$

The solid curves in Fig. 1 are the numerical solutions of the scale factor  $a$ , the Hubble parameter  $H$ , and the comoving Hubble radius  $|H^{-1}/a|$ , as functions of time  $t$ . The scale factor  $a(t)$  is normalized to unity at  $t = 0$ . It shows that the universe contracts before the quantum bounce and expands after the bounce, with a turning point of  $a(0) = 1$  corresponding to  $\bar{\mu}c = \pi/2$ . We refer to the epoch before the bounce as the ‘parent universe’.

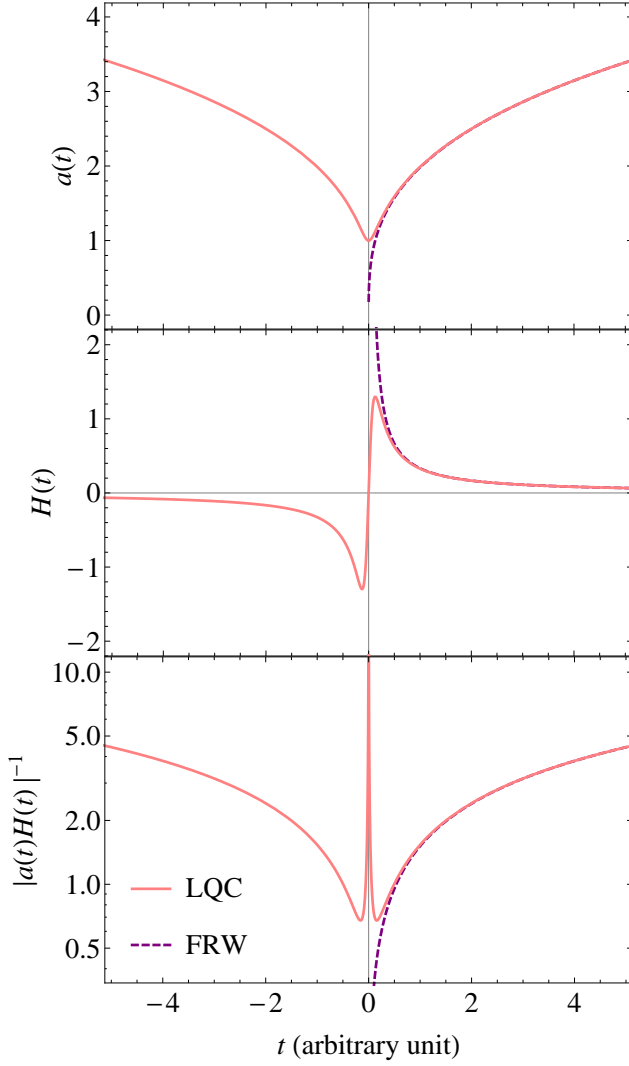


FIG. 1. The time evolution of the scale factor (top), the Hubble parameter (middle), and the comoving Hubble radius (bottom).

For the Hubble parameter, it changes its sign at the bounce. The fact that  $H(0) = 0$  indicates that the comoving Hubble radius  $|H^{-1}/a|$  diverges to infinity at the bounce. This means that the quantum effects are extremely strong such that the whole universe is in causal contact at the bounce.

The dashed curves in Fig. 1 are the results in the standard cosmology, without the quantum corrections. In this case the universe starts from singularity at  $t = 0$ , without causal connections at all because the comoving Hubble radius is zero at this time.

While the solid curves show symmetry in time with respect to the quantum bounce at  $t = 0$ , such symmetry may be broken in general cases. According to Eqs. (6), (11), (12), (13), and (14), we have

$$\frac{1}{2}\dot{\phi}^2 + V(\phi) = \rho_c^{(n)}, \quad (17)$$

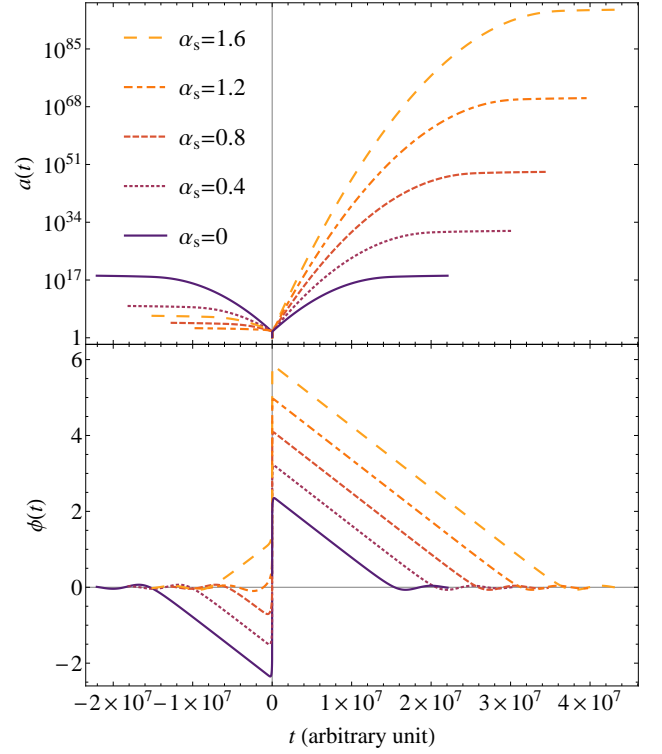


FIG. 2. The scale factor (upper panel) and the scalar field (lower panel) as functions of time at different values of  $\alpha_s$ , for Chaotic potential.

which is a constant for given  $n$ . Thus the PKR of the scalar field at the bounce is a free parameter so we may define a ‘bouncing phase’ as

$$\theta_B = \tan^{-1} \frac{\sqrt{2V(\phi)}}{\dot{\phi}}. \quad (18)$$

For the cases where  $V(\phi)$  is an even or odd function in  $\phi$ ,  $\theta_B$  determines the level of time asymmetry in the cosmic background dynamics. The case  $\theta_B = 0$  (and thus  $\phi = 0$  at bounce for the scalar-field potentials considered in this paper) corresponds to a time symmetry with respect to  $t = 0$ ; other cases lead to time asymmetry. For the cases where  $V(\phi)$  is not symmetric in  $\phi$ , the cosmic background dynamics is always asymmetric with respect to the bounce. Ref. [23] studied a special kind of asymmetric cases called the ‘shark-fin type’, which provides a relatively large number of  $e$ -foldings in the inflation after quantum bounce.

## B. The bouncing parameter

To discuss the time asymmetry in cosmic background dynamics with better accuracy, we further propose the bouncing parameter as

$$\alpha_s = \frac{-\phi(0)}{\phi_s(t_e^D)}, \quad (19)$$

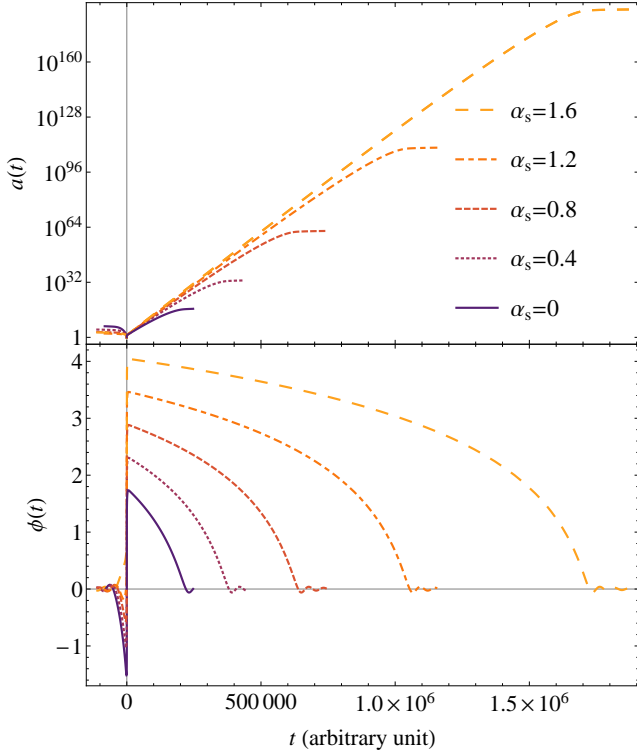


FIG. 3. The same as Fig. 2 for the  $R^2$  potential.

where  $\phi_s(t_e^D)$  is the  $\phi$  at the end of deflation  $t_e^D$  in the case with time-symmetric background. Because the number of  $e$ -foldings in inflation depends on the value of  $\phi$ , the value of  $\alpha_s$  is more directly related to the intrinsic properties of an inflationary model than  $\theta_B$ . For scalar potentials symmetric in  $\phi$ , the case  $\alpha_s = 0$  corresponds to a time-symmetric case; in a time-asymmetric case, the  $\phi_s(t_e^D)$  would differ from the  $\phi$  at the beginning of inflation leading to a non-zero  $\alpha_s$ . We note that the relation between  $\theta_B$  and  $\alpha_s$  is analytically non-trivial.

Given this formalism, we first consider the Chaotic inflation

$$V(\phi) = \frac{1}{2}m_\phi^2\phi^2. \quad (20)$$

Fig. 2 shows the scale factor and the scalar field as functions of time, at different values of  $\alpha_s$ . We have chosen the inflaton mass  $m_\phi = 10^{-6}$  in deriving the results in this figure. It is clear that  $\alpha_s = 0$  corresponds to a time-symmetric case, while a larger  $\alpha_s$  corresponds to a larger initial  $\phi$  at the beginning of inflation, leading to a larger number of  $e$ -foldings. In addition, the amount of deflation is less when  $\alpha_s$  is larger. The shark-fin type in Ref. [23] corresponds to our case with  $\alpha_s \approx 1.2$ , where the time asymmetry is about the largest. Table I shows the number of  $e$ -foldings for Chaotic inflation with various  $\alpha_s$  and  $m_\phi$ .

Next we consider the  $R^2$  inflation

$$V(\phi) = m_H^4 \left(1 - e^{-\sqrt{\frac{2}{3}}\phi}\right), \quad (21)$$

$m_\phi \backslash \alpha_s$	0	0.4	0.8	1.2	1.6
$10^{-4}$	18.5	33.0	52.2	76.0	105
$10^{-6}$	36.3	66.6	107	157	217
$10^{-8}$	60.6	113	183	270	374
$10^{-10}$	91.7	173	280	414	575

TABLE I. The number of  $e$ -foldings for inflation with Chaotic potential.

$m_\phi \backslash \alpha_s$	0	0.4	0.8	1.2	1.6
$10^{-4}$	18.5	8.45	2.56	0.33	3.66
$10^{-6}$	36.3	15.6	3.97	0.25	8.84
$10^{-8}$	60.6	25.1	5.64	0.19	16.5
$10^{-10}$	91.7	36.9	7.55	0.17	26.2

TABLE II. The number of  $e$ -foldings for deflation with Chaotic potential.

where  $m_H$  is the inflaton mass, which is normally denoted as  $\Lambda$  in literature. Here the subscript ‘H’ stands for the Higgs-like particle. The resulting time evolutions of the scale factor and the scalar field at different values of  $\alpha_s$  are presented in Fig. 3, where we have used  $m_H = 10^{-2}$ . Unlike the Chaotic inflation, here we see no case with time symmetry simply because the  $R^2$  potential is not symmetric in  $\phi$ .

These results also indicate that the cosmological inflation occurs naturally after the quantum bounce, with its initial condition unambiguously and naturally determined rather than manipulatively designed. This fact was previously studied for both time-symmetric background [22] and time-asymmetric background [23]. The four conditions required for solving the four coupled equations of motion are the Hamiltonian constraint  $H_{\bar{\mu}}^{(n)} = 0$ , the turning point condition  $\bar{\mu}c = \pi/2$ , the bouncing parameter  $\alpha_s$ , and the normalization of the scale factor  $a$ .

## IV. COSMOLOGICAL DEFLATION

### A. Quantifying Deflation

When we look into the epoch right before the quantum bounce, the scalar field may induce a damped contraction of the space, which we call the ‘cosmological deflation’. During the deflation, we have

$$\dot{a} < 0, \quad \ddot{a} > 0. \quad (22)$$

In contrast to inflation, the comoving Hubble radius grows with time during deflation. In other words, the size of causally contacted region is increasing. In addition, the energy densities and thus the perturbations are increasing. All these may counteract the inflationary

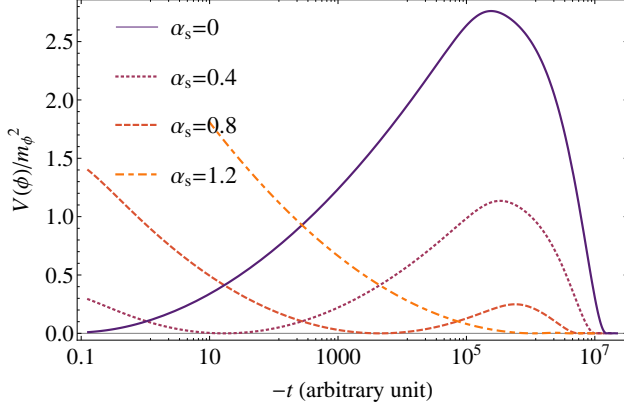


FIG. 4. Evolution of the normalized Chaotic potential before quantum bounce. The time goes leftwards in the figure, with the bounce as its origin.

effects that we need for resolving the cosmological conundrums, so a scenario with comparably less deflation is in general needed. This in turn requires asymmetry in time with respect to the quantum bounce.

Most of the formalisms used for the study of inflation are equally useful for the study of deflation, for example, the slow-roll approximation. Fig. 4 shows how the Chaotic potential evolves with time before the quantum bounce. Deflation takes place when the slope is small and thus near the peaks of the curves in the figure. For deflation we define the number of  $e$ -foldings similar to that of the inflation as

$$N_e^D \equiv \ln \left( \frac{a_b^D}{a_e^D} \right), \quad (23)$$

where  $a_b^D$  and  $a_e^D$  are the scale factors at the beginning and the end of deflation respectively. For a Chaotic potential under the slow-roll approximations, this reduces to [25]

$$N_e^D \simeq 2\pi [\phi(t_e^D)]^2 - \frac{1}{2} = 4\pi \frac{V(\phi(t_e^D))}{m_\phi^2} - \frac{1}{2}. \quad (24)$$

Combining this with Fig. 4, we see the dependence of  $N_e^D$  on  $\alpha_s$ . The dependence of  $N_e^D$  on  $m_\phi$  is implicit as  $a_b^D$  and  $a_e^D$  are dependent on  $m_\phi$ . Table II shows the dependence of  $N_e^D$  on some discrete values of  $m_\phi$  and  $\alpha_s$ . We see that for a fixed value of  $m_\phi$  the case  $\alpha_s = 1.2$  always gives the least amount of deflation, as we can also see in Fig. 4 when combined with Eq. (24). A comparison between Tables I and II also shows that the case  $\alpha_s = 0$  has the same amount of inflation and deflation so their effects are expected to be reciprocally canceled out. This is the time-symmetric case. Such scenarios are of less our interest because the cosmological conundrums revive here. In the following we shall discuss the circumstances where such cancellation can be minimized.

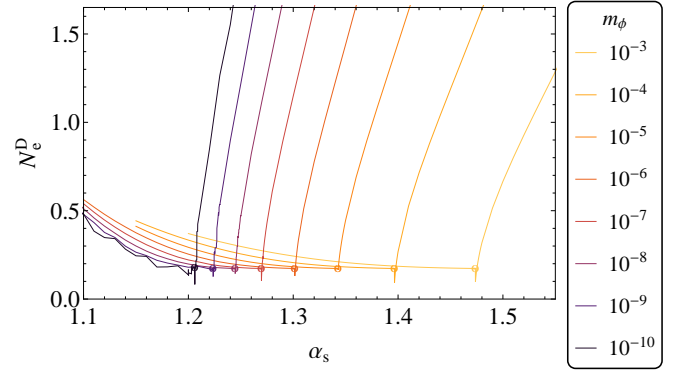


FIG. 5. The number of  $e$ -foldings  $N_e^D$  for Chaotic deflation as functions of  $\alpha_s$  for different  $m_\phi$ .

$m_\phi$	$10^{-3}$	$10^{-4}$	$10^{-5}$	$10^{-6}$	$10^{-7}$	$10^{-8}$	$10^{-9}$	$10^{-10}$
$\alpha_{\text{crit}}$	1.47	1.39	1.34	1.30	1.26	1.24	1.22	1.20

TABLE III. The values of  $\alpha_{\text{crit}}$  for different  $m_\phi$  in Chaotic deflation. They correspond to the minima in Fig. 5.

## B. Minimizing Deflation

We first numerically determine how  $N_e^D$  depends on  $\alpha_s$ . For the Chaotic potential, Fig. 5 shows the  $N_e^D$  as a function of  $\alpha_s$  at different but fixed values of  $m_\phi$ . We use  $\alpha_{\text{crit}}$  to denote the value of  $\alpha_s$  at which the minimum  $N_e^D$  occurs in a curve. Tab. III summarizes the  $\alpha_{\text{crit}}$  for different  $m_\phi$ . It is interesting to note that the minimum values of  $N_e^D$  in all cases are about the same, 0.17. We also find that  $\alpha_{\text{crit}}$  decreases with  $m_\phi$ . For each curve in Fig. 5, we note that the value of  $N_e^D$  increases more dramatically when  $\alpha_s$  departs from  $\alpha_{\text{crit}}$  to a larger value than to a smaller value.

This can be explained in Fig. 6 where we plot the comoving Hubble radius (upper panel) and the scalar field (lower panel) both as functions of time, for the case  $m_\phi = 10^{-6}$ . We consider three cases:  $\alpha_s < \alpha_{\text{crit}}$  (brown dashed),  $\alpha_s \approx \alpha_{\text{crit}}$  (orange solid), and  $\alpha_s > \alpha_{\text{crit}}$  (red dashed). In the upper panel, the parts of curves with negative slopes (increasing Hubble radius) indicate the periods when deflation takes place. These periods are shaded down to the lower panel and we see that the change in  $\phi$  during deflation is obviously larger in the case when  $\alpha_s > \alpha_{\text{crit}}$  (red dashed), resulting in the larger amount of deflation as seen in Fig. 5. We also note that in the lower panel of Fig. 6 the parts in the curves that cross  $\phi = 0$  can be thought of as the ‘inverse reheating’. This is a period when all existing articles are converted to inflaton. This epoch always takes place before the deflation, so the scenario is like a mirror process of the inflation.

For the  $R^2$  potential, the counter results are shown in Fig. 7 and Tab. IV. Again the minimum values of  $N_e^D$  in all cases are about the same, 0.15, and for a fixed  $m_H$  the amount of deflation  $N_e^D$  increases more quickly when



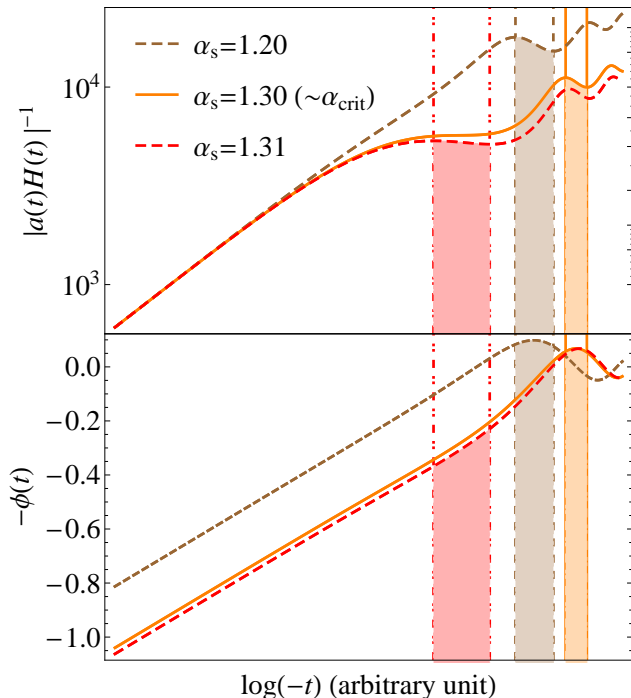


FIG. 6. The time evolution of the comoving Hubble radius (upper panel) and the scalar field (lower panel) with  $\alpha_s = 1.20$  ( $< \alpha_{\text{crit}}$ ; brown dashed),  $1.30$  ( $\approx \alpha_{\text{crit}}$ ; orange solid), and  $1.31$  ( $> \alpha_{\text{crit}}$ ; red dashed) for Chaotic potential. The vertical lines denote the beginning (right) and the end (left) of deflation, as the time goes leftwards in the plots.

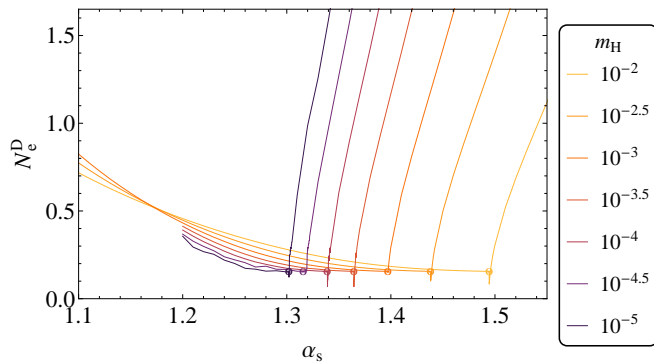


FIG. 7. The number of  $e$ -foldings  $N_e^D$  for  $R^2$  deflation as functions of  $\alpha_s$  for different  $m_H$ .

$\alpha_s$  departs from  $\alpha_{\text{crit}}$  to a larger value than to a smaller value. We verified that the reason of this is the same as discussed in Fig. 6

In summary, the amount of deflation is minimized when  $\alpha_s$  reaches  $\alpha_{\text{crit}}$ . For Chaotic potential this corresponds to the ‘most’ shark-fin type (see Fig. 2). Since this  $\alpha_s$  is model dependent and closely related to the amounts of deflation and inflation, we may use observations to confine  $\alpha_s$  and thus the model parameters.

$m_H$	$10^{-2}$	$10^{-2.5}$	$10^{-3}$	$10^{-3.5}$	$10^{-4}$	$10^{-4.5}$	$10^{-5}$
$\alpha_{\text{crit}}$	1.49	1.43	1.39	1.36	1.33	1.31	1.30

TABLE IV. The values of  $\alpha_{\text{crit}}$  for different  $m_H$  in  $R^2$  deflation. They correspond to the minima in Fig. 7.

## V. CONCLUSION

We employed the bouncing parameter  $\alpha_s$  to discuss the time asymmetry in the cosmic background evolution with respect to the quantum bounce. It is particularly noted that the time-symmetric scenarios should be avoided because in such cases deflation and inflation may counteract each other, likely leaving the cosmological conundrums unresolved. In the consideration of number of  $e$ -foldings, there is a critical value of  $\alpha_s$  at which the amount of deflation is minimized. This critical value  $\alpha_{\text{crit}}$  depends on the model parameters, namely the  $m_\phi$  and  $m_H$  in the Chaotic and  $R^2$  potentials respectively in our demonstrations. Thus when we study any model in LQC, we should be cautious about the level of time asymmetry in order to have sufficient inflation that is not pre-canceled out by the deflation before the quantum bounce. Within this context, other issues such as the cosmological perturbations also require proper treatment. In this regard we proposed a new formalism for evolving the tensor perturbations (gravitational waves) [26]. All these will need to pass the observational tests such as the cosmic microwave background in the near future.

## ACKNOWLEDGMENTS

We acknowledge the support from the Ministry of Science and Technology, Taiwan (MOST 103-2628-M-002-006-MY4).

- 
- [1] S. W. Hawking and R. Penrose, *Proceedings of the Royal Society A* **314**, 529 (1970).
  - [2] M. Bojowald, *Classical and Quantum Gravity* **19**, 30 (2002), arXiv:0202077 [gr-qc].
  - [3] M. Bojowald, *Physical Review Letters* **86**, 5227 (2001), arXiv:0102069 [gr-qc].
  - [4] A. Ashtekar, T. Pawłowski, and P. Singh, *Physical Review D* **74**, 084003 (2006), arXiv:0602086 [gr-qc].
  - [5] A. Ashtekar, T. Pawłowski, and P. Singh, *Physical Review D* **73**, 124038 (2006), arXiv:0604013 [gr-qc].

- [6] A. Ashtekar, T. Pawłowski, and P. Singh, Physical Review Letters **96**, 141301 (2006).
- [7] M. Bojowald, Living Reviews in Relativity **8**, 11 (2005).
- [8] K. Vandersloot, Physical Review D **71**, 103506 (2005).
- [9] M. Bojowald, Classical and Quantum Gravity **18**, L109 (2001).
- [10] P. Singh and K. Vandersloot, Physical Review D **72**, 084004 (2005).
- [11] D.-W. Chiou and L.-F. Li, Physical Review D **79**, 063510 (2009), arXiv:0901.1757.
- [12] D.-W. Chiou and L.-F. Li, Physical Review D **80**, 043512 (2009), arXiv:0907.0640.
- [13] M. Bojowald, Physical Review D **64**, 084018 (2001).
- [14] M. Bojowald, Physical Review Letters **89**, 261301 (2002), arXiv:0206054 [gr-qc].
- [15] A. H. Guth, Physical Review D **23**, 347 (1981).
- [16] J. Martin, C. Ringeval, R. Trotta, and V. Vennin, Journal of Cosmology and Astroparticle Physics **03**, 039 (2014).
- [17] J. F. Barbero, Physical Review D **51**, 5507 (1995), arXiv:9410014 [gr-qc].
- [18] G. Immirzi, Classical and Quantum Gravity **14**, L177 (1997).
- [19] K. A. Meissner, Classical and Quantum Gravity **21**, 5245 (2004).
- [20] Muphrid, “Hamiltonian constraint in spherical Friedmann cosmology” Stack Exchange.
- [21] J. Grain, A. Barrau, T. Cailleteau, and J. Mielczarek, Physical Review D **82**, 123520 (2010), arXiv:1011.1811.
- [22] D. W. Chiou and K. Liu, Physical Review D **81**, 063526 (2010), arXiv:1002.2035.
- [23] J. Mielczarek, T. Cailleteau, J. Grain, and A. Barrau, Physical Review D **81**, 104049 (2010).
- [24] T. Thiemann, Classical and Quantum Gravity **15**, 839 (1998), arXiv:9606090 [gr-qc].
- [25] J.-H. P. Wu, *Analytical and Numerical Approaches to Inflationary Cosmology*, M.Sc. Thesis, University of Sussex (1996).
- [26] W.-H. L. Chang and J.-H. P. Wu, (2018), arXiv:1806.10508 [gr-qc].